



Changes in the cocoa shell dietary fiber and phenolic compounds after extrusion determine its functional and physiological properties

Vanesa Benítez^{a,b}, Miguel Rebollo-Hernanz^{a,b}, Cheyenne Braojos^{a,b}, Silvia Cañas^{a,b}, Alicia Gil-Ramírez^{a,b}, Yolanda Aguilera^{a,b}, María A. Martín-Cabrejas^{a,b,*}

^a Department of Agricultural Chemistry and Food Science, Faculty of Science, C/ Francisco Tomás y Valiente, 7. Universidad Autónoma de Madrid, 28049, Madrid, Spain

^b Institute of Food Science Research (CIAL, UAM-CSIC). C/ Nicolás Cabrera, 9. Universidad Autónoma de Madrid, 28049, Madrid, Spain

ARTICLE INFO

Handling Editor: Dr. Maria Corradini

Keywords:

Cocoa shell
Extrusion
Dietary fiber
Phenolic compounds
Hypoglycemic properties
Hypolipidemic properties

ABSTRACT

The influence of different extrusion conditions on the cocoa shell (CS) dietary fiber, phenolic compounds, and antioxidant and functional properties was evaluated. Extrusion produced losses in the CS dietary fiber (3–26%), especially in the insoluble fraction, being more accentuated at higher temperatures (160 °C) and lower moisture feed (15–20%). The soluble fiber fraction significantly increased at 135 °C because of the solubilization of galactose- and glucose-containing insoluble polysaccharides. The extruded CS treated at 160 °C–25% of feed moisture showed the highest increase of total (27%) and free (58%) phenolic compounds, accompanied by an increase of indirect (10%) and direct (77%) antioxidant capacity. However, more promising results relative to the phenolic compounds' bioaccessibility after *in vitro* simulated digestion were observed for 135 °C–15% of feed moisture extrusion conditions. The CS' physicochemical and techno-functional properties were affected by extrusion, producing extrudates with higher bulk density, a diminished capacity to hold oil (22–28%) and water (18–65%), and improved swelling properties (14–35%). The extruded CS exhibited increased glucose adsorption capacity (up to 2.1-fold, at 135 °C–15% of feed moisture) and α -amylase *in vitro* inhibitory capacity (29–54%), accompanied by an increase in their glucose diffusion delaying ability (73–91%) and their starch digestion retardation capacity (up to 2.8-fold, at 135 °C–15% of feed moisture). Moreover, the extruded CS preserved its cholesterol and bile salts binding capacity and pancreatic lipase inhibitory properties. These findings generated knowledge of the CS valorization through extrusion to produce foods rich in dietary fiber with improved health-promoting properties due to the extrusion-triggered fiber solubilization.

1. Introduction

Cocoa (*Theobroma cacao* L.) processing produces a variety of by-products, being the cocoa shell (CS) the main one. The CS, also known as hull and husk, is the outer section of cocoa beans that holds the nibs. It is removed after the roasting process during chocolate production (Belwal et al., 2022). The CS represents 12–20% of cocoa seeds, and its annual production is estimated at around 600,000 tons (Boeckx et al., 2020). Conventionally, the CS has been used as fuel in cocoa processing facilities or organic matter to supply soil nutrients and fight weeds. Other applications proposed include using the CS as animal feed, adsorbent, or biofiltration agent for the food industry wastewater (Rebollo-Hernanz et al., 2022a). The biorefinery of cocoa processing by-products into valuable goods is increasing attention. Consequently,

industrial countries are developing strategic policies to transition toward a circular bioeconomy (Kumar et al., 2022).

Current research focuses on novel food applications of the CS due to its comparable chocolate sensorial properties and excellent nutritional value (Belwal et al., 2022). The CS has been included in foods, such as bread, biscuits, and muffins, with positive results on the sensory qualities of these new products (Nogueira Soares Souza et al., 2022). The CS is rich in dietary fiber and other phytochemicals, such as theobromine and phenolic compounds. As a result of this composition, the CS exhibits hypoglycemic and hypolipidemic properties observed *in vitro*, in cell culture models, and *in vivo* (Rebollo-Hernanz et al., 2019, 2022b). Dietary fiber in the CS comprises a complex polysaccharide structure embedding phenolic compounds that confers it enhanced antioxidant properties (Soares and Oliveira, 2022). Phenolic compounds in the CS

* Corresponding author. Institute of Food Science Research (CIAL, UAM-CSIC). C/ Nicolás Cabrera, 9. Universidad Autónoma de Madrid, 28049, Madrid, Spain.

E-mail addresses: vanesa.benitez@uam.es (V. Benítez), miguel.rebollo@uam.es (M. Rebollo-Hernanz), cheyenne.braojos@uam.es (C. Braojos), silvia.cannas@uam.es (S. Cañas), alicia.gil@uam.es (A. Gil-Ramírez), yolanda.aguilera@uam.es (Y. Aguilera), maria.martin@uam.es (M.A. Martín-Cabrejas).

<https://doi.org/10.1016/j.crfs.2023.100516>

Received 16 November 2022; Received in revised form 9 March 2023; Accepted 7 May 2023

Available online 8 May 2023

2665-9271/© 2023 The Authors. Published by Elsevier B.V. This is an open access article under the CC BY-NC-ND license (<http://creativecommons.org/licenses/by-nc-nd/4.0/>).

are released from the dietary fiber matrix during gastrointestinal digestion, being bioaccessible and potentially transformed by the gut microbiota into smaller and more bioavailable phenolic metabolites (Cañas et al., 2022). Therefore, the CS could be a suitable ingredient for formulating foods with cocoa-like sensory attributes, enriched in dietary fiber and phytochemicals that could exert broad health-promoting properties.

Extrusion could be a promising technology for including the CS in foodstuffs. Extruded-based snacks and breakfast cereals are popular, although most display low nutritional value, which has led the food industry to develop nutrient-dense, healthier, and functionalized products (Menis-Henrique et al., 2020). In this regard, incorporating the CS into food formulations could be an encouraging approach to developing novel, healthy, eco-friendly, sustainable extruded products (Grasso, 2020). However, extrusion is a thermo-mechanical short-time process involving high temperatures, pressure, and shear forces, usually resulting in physical and chemical modifications of the material, i.e., structure, texture, protein denaturalization, or polysaccharides solubilization (Leonard et al., 2020). Fibrous food by-products have been extruded, resulting in dietary fiber solubilization, phenolic compounds release from the matrix, and techno-functional and antioxidant properties modifications (García-Amezquita et al., 2019; Villasante et al., 2019). The changes mentioned above, which are intricately tied to the processing parameters, could alter the CS chemical and phytochemical composition and, as a result, modify their functionality and biological activity (Santos et al., 2022). Jozinović et al. (2019) investigated corn-CS extruded snacks' technological and texture properties. Nonetheless, no scientific evidence about the effect of extrusion on the dietary fiber composition and physiological properties of the CS has been reported.

Hence, the objective of the present work was to evaluate the modifications that occur during the extrusion process, at different conditions of temperature and moisture, on the chemical composition and functional and physiological properties of the CS. For this purpose, we analyzed the dietary fiber, phenolic compounds, antioxidant capacity, physicochemical and techno-functional, and *in vitro* hypoglycemic and hypolipidemic properties of the CS extruded at different conditions.

2. Materials and methods

2.1. Materials

The CS was supplied by Chocolates Santocildes (Castrocontrigo, León). The CS was ground in a pilot scale ball mill (Ortoalresa-Álvarez Redondo S.A., Madrid) for 72 h. Ground CS was sieved (250 µm) and stored at −20 °C until analysis.

2.2. Extrusion process

Extrusion was performed in triplicate in a lab-scale single-screw extruder (Compact E 19/25 D; Brabender, Duisburg, Germany) with a 19/25D screw, 3:1 compression ratio, and the die opening had a diameter of 3 mm. The total length of the screw was 19 mm, and the length-to-diameter ratio (L:D) was 25. The process was performed at a constant screw speed of 150 rpm and an extruder feed hopper speed of 200 rpm (yielding an estimated feed rate of 1.8 kg/h). The effect of extrusion moisture content (15, 20, and 25%) and barrel temperature ramps (135–150 °C and 160–175 °C) were investigated, obtaining a total of six different extrusion conditions and a non-extruded CS flour. The temperature in the barrel increased by 5 °C over four different zones (135 > 140 > 145 > 150 °C or 160 > 165 > 170 > 175 °C), being 150 or 175 °C the final temperature at the die. Afterward, the extruded and non-extruded CS (used as control) (Table 1) were milled and stored in sealed plastic bags at −20 °C until analysis.

Table 1

Extrusion treatment parameters (temperature and moisture) and sample code.

Sample code	Extrusion treatment	
	Temperature (°C)	Moisture (%)
Control	Non-treated	Non-treated
E135–15	135–150	15
E135–20	135–150	20
E135–25	135–150	25
E160–15	160–175	15
E160–20	160–175	20
E160–25	160–175	25

2.3. Determination of dietary fiber

The enzymatic-gravimetric method (Mes-Tris AOAC method 991.43) was used to determine the content of dietary fiber in extruded and non-extruded CS (Benítez et al., 2021). Dietary fiber fractions were obtained after enzymatic digestion, and the generated insoluble residues were isolated by filtration. Additionally, soluble fiber was precipitated from the filtrate using ethanol and isolated by filtration. Residues obtained after ash and protein correction correspond to the insoluble dietary fiber (IDF) and soluble dietary fiber. Total dietary fiber (TDF) resulted from the sum of the IDF and the SDF.

2.4. Determination of dietary fiber composition

The composition of the dietary fiber fractions was determined after acid hydrolysis of the residues obtained in section 2.3. Briefly, insoluble fiber residues were subjected to 12 M H₂SO₄ treatment for 3 h at room temperature followed by dilution to 0.6 M H₂SO₄ hydrolysis at 100 °C for 3 h (Seaman hydrolysis) and to a 0.6 M H₂SO₄ hydrolysis at 100 °C for 3 h. Soluble fiber residues were hydrolyzed only with 0.6 M H₂SO₄ at 100 °C for 3 h. Afterward, the fiber components, i.e., neutral sugars, uronic acids, and Klason lignin, were quantified (Benítez et al., 2019). The neutral sugars composition in the CS dietary fiber fractions was determined by HPLC-PAD. The concentration of uronic acids was determined using a commercial kit (K-URONIC, Megazyme Co. Wicklow, Ireland) following the manufacturer's instructions. Cellulose and non-cellulosic polysaccharides (NCP) were estimated from their corresponding individual sugar contents.

2.5. Extraction and determination of free, bound, and total phenolics

Free and bound phenolic compounds (FPC and BPC, respectively) were extracted from the non-extruded and extruded CS using methanol: HCl: water (79.5: 0.5: 20) as previously described (Rebollo-Hernanz et al., 2021). FPC and BPC were analyzed by the Folin-Ciocalteu method using gallic acid as standard. The results were expressed as mg/g gallic acid equivalents (GAE). Total phenolic compounds (TPC) derived from the sum of FPC and BPC.

2.6. Overall antioxidant capacity

Overall antioxidant capacity was measured by both direct and indirect ABTS assay, according to Benítez et al. (2019). Direct ABTS (direct AC) was evaluated in the extruded and non-extruded CS, and indirect ABTS (indirect AC) was measured in the FPC and BPC extracts (AC-FPC and AC-BPC). Total indirect antioxidant capacity (AC-TPC) was calculated by adding the AC-FPC to the AC-BPC. Trolox was used as standard, and the results were expressed as mg/g Trolox equivalents (TE).

2.7. Release of phenolic compounds and their antioxidant capacity during *in vitro* simulated digestion

2.7.1. Simulated *in vitro* digestion

Gastrointestinal digestion was performed following the harmonized INFOGEST protocol to evaluate the release of phenolic compounds from the extruded and non-extruded CS (Brodtkorb et al., 2019). The supernatants and non-digestible residues (ND) from the gastric and gastrointestinal phases (GP, IP, NDG, and NDI, respectively) were lyophilized and stored at -20°C until further use.

2.7.2. Determination of released and non-digested phenolic compounds and their *in vitro* antioxidant capacity

The content of released phenolic compounds (RPC) and their antioxidant capacity (AC-RPC) were determined in gastric (RPC-G) and gastrointestinal (RPC-I) supernatants, as previously described in section 2.5. Moreover, phenolic bioaccessibility was calculated in the gastrointestinal phase regarding FPC or TPC, as follows:

$$\text{Bioaccessibility (\%)} = \frac{[\text{RPC} - \text{I}]}{[\text{FPC}] \text{ or } [\text{TPC}]} \times 100$$

Similarly, the AC-recovery index was calculated using the AC values of the corresponding fractions.

The residues of each phase, gastric and gastrointestinal, were subjected to the extraction and determinations described in sections 2.5 and 2.6 to evaluate the content of FPC, BPC, and TPC in the ND of the gastric and gastrointestinal phases (FPC-NDG, BPC-NDG, and TFC-NDG; FPC-NDI, BPC-NDI, and TFC-NDI, respectively) and their antioxidant capacity (AC-FPC-NDG, AC-BPC-NDG, and AC-TFC-NDG; AC-FPC-NDI, AC-BPC-NDI, and AC-TFC-NDI, respectively). The results were expressed as mg GAE or mg TE/g of CS.

2.8. Techno-functional properties

pH was measured according to the official AOAC procedure. Bulk density (BD), oil holding capacity (OHC), water holding capacity (WHC), water absorption capacity (WAC), swelling capacity (SWC), and emulsifying activity (EA) were determined according to Benítez et al. (2019).

2.9. *In vitro* hypoglycemic properties

2.9.1. Glucose-adsorption capacity

Glucose-adsorption capacity was determined by mixing the extruded CS with different concentrations of glucose (10, 50, 100, 200 mM), according to Benítez et al. (2019). The amount of glucose adsorbed was evaluated using a commercial kit (K-GLUC, Megazyme, Wicklow, Ireland). The results were expressed as mmol adsorbed glucose/g of CS. The maximum amount of adsorbed glucose was calculated by obtaining the (second-order) curve's maximum.

2.9.2. Amylase inhibition capacity

The residual α -amylase activity was evaluated according to Benítez et al. (2019). Briefly, non-extruded and extruded CS were incubated with α -amylase (Sigma-Aldrich, MO, USA) and a 4% potato starch solution to evaluate starch degradation, followed by enzyme inactivation and centrifugation steps. Glucose content was quantified in the supernatant, and results were expressed as a percentage of inhibition regarding the maximum glucose produced in the absence of non-extruded or extruded CS.

2.9.3. Capacity to retard glucose diffusion

In vitro glucose diffusion was evaluated by determining the kinetics of glucose dialysis in the presence or absence (blank) of samples for 10, 30, 60, 90, 120, and 150 min of incubation time. Afterward, glucose was quantified in the dialysate using the K-GLUC kit (Benítez et al., 2021).

The maximum glucose diffusion rate (V_{max} glucose diffusion) was calculated by fitting the experimental data to a second-order equation:

$$Y \text{ (Dialyzed glucose, } \mu\text{mol)} = at^2 + bt + c$$

where a , b , and c are the coefficients and t is the diffusion time (min). The first derivative of the equation was used to calculate the diffusion rate (Y'). Since $Y' = 2at + b$, when t is close to 0, $Y' = V_{\text{max}} = b$. The capacity of samples to retard glucose diffusion was calculated using the glucose diffusion retardation index (GDRI):

$$\text{GDRI} = 100 - \frac{[\text{Glucose}] \text{ in the dialysate with CS addition}}{[\text{Glucose}] \text{ in the dialysate of blank test}} \times 100$$

2.9.4. Capacity to retard starch digestibility

Starch digestibility was evaluated according to Benítez et al. (2021). Briefly, a mixture of samples, α -amylase, and potato starch solution was dialyzed against distilled water. After incubation, glucose was determined in the dialysate using the K-GLUC kit. A control experiment (blank) was performed without the addition of samples. The maximum diffusion rate for the hydrolyzed starch (V_{max} starch hydrolysis) and the capacity to retard the starch digestibility (GDRI-starch hydrolysis) were calculated as described in section 2.9.3.

2.10. *In vitro* hypolipidemic properties

2.10.1. Cholesterol binding capacity

Cholesterol absorption capacity was determined according to Benítez et al. (2021). A mixture of non-extruded or extruded CS with diluted egg yolk was incubated (37°C , 2 h) after adjusting its pH to 2.0 or 7.0. Then, samples were centrifuged, and the supernatants were diluted with acetic acid (90% v/v), mixed with *o*-phthalaldehyde, and incubated for color development. Results were expressed as the percentage of bound cholesterol compared to a control test without samples (blank).

2.10.2. Bile salts' binding capacity

The bile salts' absorption capacity was evaluated according to Benítez et al. (2021). Samples were mixed with a NaCl solution and sodium cholate (Sigma-Aldrich, MO, USA), followed by a gentle stirring for 1 or 3 h before centrifugation. Binding capacity was determined by comparing the concentration of sodium cholate before and after the reaction time. After incubation, supernatants were recovered and mixed with H_2SO_4 (45% v/v) and furfural (0.3% v/v), followed by incubation and cooling at room temperature (25°C).

2.10.3. Lipase inhibition capacity

The ability of studied samples for pancreatic lipase inhibition was determined by incubating a mixture of non-extruded or extruded CS, olive oil, sodium phosphate buffer (0.1 M, pH 7.2), and pancreatic lipase for 1 h in the presence or absence of bile salts (Benítez et al., 2021). Once the reaction was stopped by a heat shock (100°C , 5 min), the hydrolysis of triglycerides and production of free fatty acids were analyzed by titrating with NaOH (0.05 M). A similar procedure without adding CS was used as reaction control (blank). The enzyme inhibitory activity (%) was defined as the decrease of free fatty acid production compared to the blank.

2.11. Statistical analysis

Sample analyses were performed in triplicate. The data were analyzed by *T*-test or one-way analysis of variance (ANOVA) and post hoc Tukey's test using SPSS 26.0. Pearson's linear correlation coefficients were calculated to evaluate the relationships between the analyzed parameters at $p < 0.05$, $p < 0.01$, and $p < 0.001$ levels of significance. A hierarchical cluster analysis was performed using XLSTAT 2020 for Microsoft Excel 2016.

3. Results and discussion

3.1. Changes in the proportion of soluble: insoluble dietary fiber in the cocoa shell after extrusion

The CS exhibited a high content of dietary fiber, mainly IDF (48.6%) and low SDF (10.5%) (Fig. 1A). Extrusion produced significant ($p < 0.05$) losses of TDF at 160 °C–15% moisture (26%) and 160 °C–20% moisture (15%) due to the noticeable reduction of IDF in these conditions (28 and 15%, respectively) (Fig. 1A and B). Additionally, the SDF significantly increased when the extrusion was performed at 135 °C, from 10% at 135 °C–25% moisture to 35% at 135 °C–15% moisture, which explains why the TDF did not change at 135 °C. No differences were found in the SDF at 160 °C. These SDF increases at 135 °C could be partially due to the transformation of certain IDF into SDF during extrusion. Even though changes in the dietary fiber after extrusion might depend on the food matrix and the extrusion process parameters, losses in the content of one of the dietary fiber fractions without altering the other fraction have been previously reported (Leonard et al., 2020). Then, both fractions could have been degraded at higher temperatures (160 °C) since extrusion produces chemical reactions, especially the breakdown of polymeric compounds. Thus, part of the CS dietary fiber could have been solubilized or broken into lower molecular weight fragments or soluble sugars during extrusion (Bader Ul Ain et al., 2019). A higher degradation is associated with low moisture feed due to a greater mechanical shear (Espinosa-Ramírez et al., 2021). Nevertheless, no significant differences were observed among the three moisture levels within the same temperature groups. The decrease in the content of dietary fiber and its solubilization produced extruded CS with slightly less fiber content but a better SDF: IDF ratio (1:3–1:4) compared to the non-extruded CS (1:5) (Fig. 1B). Generally, fiber sources suitable to be included as food ingredients should depict SDF: IDF ratio close to 1: 3, wherein the insoluble fraction is in the majority, to provide the physiological effects associated with both fractions (Bader Ul Ain et al., 2019).

3.2. Low-temperature extrusion enriched the cocoa shell's soluble dietary fiber in galactose- and glucose-containing polysaccharides

The polysaccharides present in the CS' IDF were mainly constituted of glucose (47–58%), followed by notable contents of uronic acids, galactose, xylose, and arabinose, whereas mannose and rhamnose occurred in lower content (Table 2). In origin, glucose content was mainly cellulosic since 0.6 M H₂SO₄ released less than 10%. Then, cellulose was inferred to be the primary cell wall polysaccharide in IDF (16–24%), followed by non-cellulosic polysaccharides (NCP, hemicelluloses and pectic substances) (16–23%) (Fig. 1C). Interestingly, uronic acids, galactose, and arabinose were found at the same or higher levels in 0.6 M hydrolysis than in sequential hydrolysis (Seaman, 12 + 0.6 M H₂SO₄), whereas xylose was released at lower levels. These results pinpoint that the cellulosic matrix was intimately related to hemicelluloses (presumably xyloglucans). In contrast, homogalacturonans and neutral pectic polysaccharides such as arabinans, galactans, and arabinogalactans exhibited weaker linkages to the cellulosic matrix.

Extrusion yielded modifications in the composition of the CS' IDF, mainly associated with the temperature of the process. The IDF fraction in the extruded CS exhibited a significant ($p < 0.05$) lower total sugar content (172–200 mg/g), which provides an overview of the cellulosic and non-cellulosic polysaccharides, than the non-extruded CS (230 mg/g), mainly due to the decreases of glucose, xylose, galactose, arabinose, and uronic acids, being higher at 160 °C than at 135 °C, except for glucose (Fig. 1C, Table 2). Extrusion induces the loss of cellulose and the decrease of hemicelluloses and pectic substances depending on the extrusion temperature (Schmid et al., 2020). In addition, results showed that extrusion significantly ($p < 0.05$) increased lignin content at 135 °C–20% moisture (8%) and 135 °C–25% moisture (16%) but significantly ($p < 0.05$) diminished at 160 °C–15% moisture (40%) and 160 °C–20% moisture (10%), reaching a maximum of 219.9 mg/g at 135 °C with 25% moisture feed.

The SDF fraction was mainly composed of uronic acids (36–50%) and galactose (33–39%), followed by arabinose, glucose, mannose, and rhamnose (Table 2). Therefore, homogalacturonans and neutral galactose pectic polysaccharides would be the main polysaccharides of the SDF in the extruded CS. Extrusion significantly ($p < 0.05$) increased the neutral and total sugar content except for 160 °C and 25% moisture feed, whose SDF sugars were like those from the non-extruded CS. The increases were mainly due to galactose and, in less extent, glucose, probably derived from the solubilization of the IDF fraction, as previously reported (Menis-Henrique et al., 2020). Taken together, the TDF composition of the extruded CS indicated that extrusion generated a higher loss of galactose, xylose, arabinose, mannose, and uronic acids at 160 than 135 °C, corroborating the greater degradation found at a higher temperature (160 °C) by the gravimetric method and the redistribution of IDF to SDF at 135 °C.

3.3. Extrusion of the cocoa shell at high temperatures and high moisture increased the concentration of phenolic compounds and the antioxidant capacity

The effect of extrusion on phenolic compounds depends on extrusion parameters and matrix composition (Yi et al., 2022). The CS extruded at 160 °C–25% of feed moisture showed a significantly ($p < 0.05$) higher TPC (27%) and FPC (58%) content compared with the non-extruded CS, unlike the other conditions (Table 3). However, a significant reduction in the BPC (50 and 60%) occurred when extrusion was performed at 15% moisture feed moisture at 135 °C and 160 °C, respectively. Such extrusion parameters may assist the release of phenolic compounds from the food matrix, mainly conjugated phenolics, which were covalently bound to the insoluble fiber fraction (Rani et al., 2018). The TPC tended to increase with temperature and moisture feed. The CS extruded at 25% moisture feed (independently of the temperature) showed a significantly ($p < 0.05$) higher TPC (45–50%) than those extruded at 15% moisture. These results revealed that high moisture content might protect these bioactive compounds, avoiding their friction losses.

The increase in the total phenolic content as a result of moisture conditions could be responsible for the significantly ($p < 0.05$) higher indirect AC observed with 25% moisture content at both temperatures

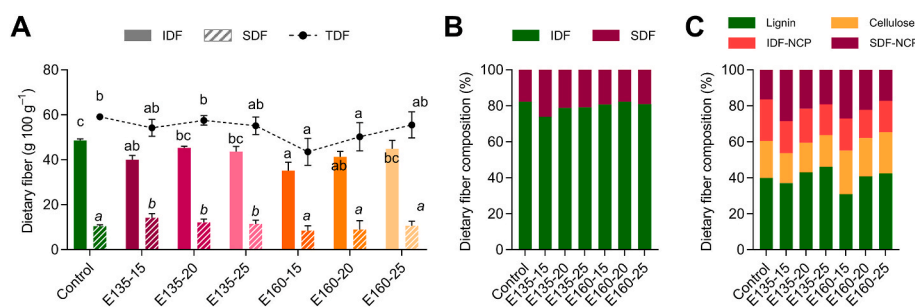


Fig. 1. Influence of extrusion on the content of dietary fiber measured by the gravimetric method (A) and fiber fractions proportions according to solubility (B) and chemical composition (C) in the cocoa shell under different temperature (135–150 or 160–175 °C) and moisture (15, 20, or 25%) processing conditions. The results are reported as mean \pm SD ($n = 3$). Bars and points with different letters significantly ($p < 0.05$) differ according to ANOVA and Tukey's multiple range test. IDF: Insoluble Dietary Fiber; SDF: Soluble Dietary Fiber; NCP: Non-Cellulosic Polysaccharides.

Table 2

Monosaccharide composition of the IDF and SDF fractions from non-extruded and extruded cocoa shell (mg/g).

	DF Fraction	Hydrolysis	Neutral monosaccharides						Total neutral sugars	AU	Total sugars	Klason Lignin	IDF or SDF†	TDF‡
			Glu	Gal	Xyl	Ara	Man	Rha						
Control	IDF	Seaman	108.2 ± 0.2 ^b	22.3 ± 1.2 ^c	20.7 ± 0.3 ^d	20.7 ± 0.4 ^c	10.9 ± 0.1 ^c	2.4 ± 0.1 ^b	185.3 ± 2.3 ^c	36.8 ± 2.1 ^d	230.3 ± 5.3 ^b	189.3 ± 3.1 ^c	419.6 ± 8.4 ^c	506.4 ± 12.9 ^b
		0.6 M	6.6 ± 25.1	25.1 ± 5.8 ^y	3.2 ± 23.9	1.4 ± 23.9	1.4 ± 1.3	1.3 ± 61.5	45.0 ± 3.0 ^x	45.0 ± 3.0 ^x				
		H ₂ SO ₄	0.4 ^z	± 5.8 ^y	1.3 ^z	± 0.4 ^z	0.3 ^z	0.4 ^z	8.6 ^y	± 3.0 ^x				
	SDF	0.6 M	3.4 ±	30.0	–	3.2 ±	5.6 ±	3.7 ±	46.0 ±	40.9	86.8 ±		86.8 ±	
		H ₂ SO ₄	0.4 ^b	± 2.0 ^a		0.5 ^a	0.5 ^b	0.1 ^b	2.4 ^a	± 2.1 ^a	4.5 ^a		4.5 ^a	
E135–15	IDF	Seaman	87.9 ± 0.7 ^a	15.9 ± 0.9 ^b	18.3 ± 1.8 ^c	15.1 ± 1.1 ^b	8.6 ± 1.2 ^b	1.7 ± 0.1 ^a	147.6 ± 6.9 ^a	31.9 ± 1.3 ^c	181.8 ± 9.2 ^a	175.3 ± 12.7 ^b	357.1 ± 21.8 ^b	506.6 ± 28.2 ^b
		0.6 M	8.4 ±	18.3	2.3 ±	21.8	1.3 ±	1.5 ±	53.6 ±	34.2				
		H ₂ SO ₄	0.4 ^y	± 2.5 ^z	0.5 ^z	± 6.6 ^z	0.1 ^z	0.3 ^{zy}	10.4 ^z	± 2.3 ^y				
	SDF	0.6 M	13.1 ±	58.3	–	8.6 ±	7.7 ±	7.4 ±	95.1 ±	54.4	149.5 ±		149.5 ±	
		H ₂ SO ₄	0.8 ^f	± 1.2 ^c		0.3 ^c	0.9 ^c	0.0 ^f	3.2 ^d	± 3.1 ^b	6.3 ^c		6.3 ^c	
E135–20	IDF	Seaman	87.0 ± 8.0 ^a	15.6 ± 1.0 ^b	17.9 ± 1.2 ^c	15.2 ± 1.5 ^b	9.0 ± 0.9 ^b	3.9 ± 0.7 ^c	148.3 ± 13.3 ^a	33.6 ± 2.1 ^{cd}	187.1 ± 15.0 ^a	205.0 ± 9.0 ^d	392.1 ± 23.9 ^{bc}	506.3 ± 31.8 ^b
		0.6 M	8.0 ±	20.4	6.1 ±	26.9	1.6 ±	1.8 ±	65.1 ±	38.6				
		H ₂ SO ₄	0.2 ^y	± 0.1 ^y	0.8 ^y	± 1.3 ^z	0.3 ^z	0.1 ^y	2.8 ^y	± 1.7 ^y				
	SDF	0.6 M	11.0 ±	43.0	–	4.8 ±	6.2 ±	6.4 ±	71.3 ±	43.0	114.3 ±		114.3 ±	
		H ₂ SO ₄	0.2 ^e	± 4.2 ^b		0.4 ^b	0.5 ^b	0.2 ^e	5.5 ^c	± 2.4 ^a	7.9 ^b		7.9 ^b	
E135–25	IDF	Seaman	92.9 ± 4.2 ^a	13.0 ± 3.4 ^{ab}	11.2 ± 1.3 ^a	14.4 ± 1.8 ^b	6.4 ± 1.6 ^a	1.8 ± 0.3 ^a	139.7 ± 12.6 ^a	33.5 ± 1.9 ^{cd}	184.0 ± 14.6 ^a	219.9 ± 19.3 ^d	403.9 ± 33.9 ^c	504.9 ± 44.2 ^b
		0.6 M	7.9 ±	20.3	6.3 ±	26.9	1.5 ±	2.2 ±	65.1 ±	44.2				
		H ₂ SO ₄	0.7 ^y	± 2.1 ^y	1.9 ^y	± 2.5 ^z	0.6 ^z	0.4 ^y	9.2 ^y	± 2.0 ^x				
	SDF	0.6 M	7.1 ±	39.2	–	2.8 ±	6.2 ±	5.6 ±	60.9 ±	40.1	101.0 ±		101.0 ±	
		H ₂ SO ₄	0.4 ^d	± 5.7 ^b		0.7 ^a	0.4 ^b	0.3 ^d	7.5 ^b	± 2.8 ^a	10.3 ^b		10.3 ^{ab}	
E160–15	IDF	Seaman	99.9 ± 4.1 ^{ab}	10.8 ± 2.5 ^a	14.8 ± 1.9 ^b	11.0 ± 0.3 ^a	7.8 ± 1.9 ^{ab}	3.1 ± 0.2 ^c	147.4 ± 10.9 ^a	20.9 ± 1.5 ^a	173.6 ± 12.3 ^a	114.1 ± 4.5 ^a	287.7 ± 16.8 ^a	398.3 ± 23.2 ^a
		0.6 M	8.0 ±	20.4	6.9 ±	27.2	1.7 ±	1.8 ±	65.4 ±	26.1				
		H ₂ SO ₄	0.0 ^y	± 4.2 ^y	1.3 ^y	± 1.9 ^z	0.6 ^z	0.0 ^y	8.0 ^y	± 1.4 ^z				
	SDF	0.6 M	6.2 ±	36.8	–	4.6 ±	8.3 ±	6.7 ±	62.5 ±	48.2	110.7 ±		110.7 ±	
		H ₂ SO ₄	0.4 ^d	± 2.0 ^b		0.3 ^b	0.2 ^c	0.3 ^{ef}	3.2 ^b	± 3.3 ^{ab}	6.5 ^b		6.5 ^b	
E160–20	IDF	Seaman	99.4 ± 8.5 ^{ab}	9.2 ± 2.6 ^a	10.4 ± 3.7 ^a	11.3 ± 3.7 ^a	7.0 ± 1.6 ^a	1.7 ± 0.8 ^a	139.0 ± 20.9 ^a	28.1 ± 1.7 ^b	172.1 ± 22.7 ^a	170.8 ± 5.3 ^b	342.9 ± 28.1 ^b	446.4 ± 32.8 ^{ab}
		0.6 M	8.1 ±	21.0	6.4 ±	26.1	1.6 ±	1.5 ±	65.1 ±	33.0				
		H ₂ SO ₄	0.1 ^y	± 0.5 ^y	1.2 ^y	± 1.6 ^z	0.3 ^z	0.1 ^{zy}	3.8 ^y	± 1.8 ^y				
	SDF	0.6 M	4.5 ±	38.4	–	4.3 ±	6.6 ±	4.7 ±	58.5 ±	44.9	103.4 ±		103.4 ±	
		H ₂ SO ₄	0.1 ^c	± 1.1 ^b		0.1 ^b	0.1 ^b	0.2 ^c	1.6 ^b	± 3.1 ^a	4.7 ^b		4.7 ^{ab}	
E160–25	IDF	Seaman	113.6 ± 2.8 ^b	11.6 ± 0.1 ^a	16.5 ± 0.5 ^{bc}	11.0 ± 1.0 ^a	9.3 ± 1.7 ^b	3.1 ± 0.4 ^c	165.2 ± 7.7 ^b	28.7 ± 2.0 ^b	200.3 ± 10.2 ^a	189.6 ± 3.2 ^c	389.9 ± 13.4 ^{bc}	475.1 ± 19.8 ^b
		0.6 M	10.6 ±	30.2	15.4	24.1	2.9 ±	2.6 ±	85.9 ±	35.1				
		H ₂ SO ₄	0.5 ^x	± 8.3 ^x	± 2.5 ^x	± 0.1 ^z	0.1 ^y	0.0 ^x	11.5 ^x	± 2.5 ^y				
	SDF	0.6 M	2.2 ±	32.5	–	3.6 ±	2.5 ±	2.2 ±	42.9 ±	42.3	85.2 ±		85.2 ±	
		H ₂ SO ₄	0.4 ^a	± 2.1 ^a		0.2 ^a	0.7 ^a	0.4 ^a	3.8 ^a	± 2.6 ^a	6.4 ^a		6.4 ^a	

Results are reported as mean ± SD ($n = 3$). Mean values within the same column, DF fraction, and hydrolysis conditions, followed by different superscript letters (a, b, c ...) indicate differences between samples IDF-Saeman hydrolysis (within the same column); superscript letters (z, y, x ...) indicate differences between samples IDF-0.6M H₂SO₄ hydrolysis (within same column); and subscript letter (a, b, c ...) indicate differences between samples SDF-0.6M H₂SO₄ hydrolysis (within the same column) once subjected to Tukey's test ($p < 0.05$). IDF: Insoluble Dietary Fiber; SDF: Soluble Dietary Fiber; TDF: Total Dietary Fiber; Glu: Glucose; Gal: Galactose; Xyl: Xylose; Ara: Arabinose; Man: Mannose; Rha: Rhamnose; UA: Uronic Acids. †Chemical IDF and SDF calculated as the sum of its components ‡Chemical TDF calculated as the sum of chemical IDF and SDF.

(37.7 mg TE/g) compared to CS extruded with 15% moisture at 135 °C (26.8 mg TE/g) and 160 °C (29.3 mg TE/g) (Table 3). Only the CS extruded at 25% moisture feed at both temperatures displayed a significantly higher (10%, $p < 0.05$) indirect AC compared to the non-extruded CS (34.4 mg TE/g), while the opposite trend was observed for a 15% moisture feed at both temperatures. This behavior would probably be due to the loss of bound phenolic compounds exhibited with the low moisture barrel feed ($r = 0.734$, $p < 0.05$) (Fig. 2A). The CS's *in vitro* and *ex vivo* antioxidant properties were previously assigned to phenolic compounds, mainly to protocatechuic acid, the main compound bound to the dietary fiber matrix (Rebollo-Hernanz et al., 2021; Rodríguez-Rodríguez et al., 2022; Cañas et al., 2023). Here we corroborated the association of the total indirect AC and the quantified total phenolic compounds ($r = 0.921$, $p < 0.05$). Nevertheless, other compounds might be participating in the antioxidant capacity of the extruded and non-extruded CS, as samples exhibited higher direct than

indirect AC (determined in the phenolic extracts) (Table 3). These compounds could correspond to other CS components, such as proteins, aromatic compounds, pigments, or processing-derived ones, such as antioxidant melanoidins, produced through the Maillard reaction due to the high temperatures (Yi et al., 2022). Results indicated a positive correlation between direct antioxidant capacity with temperature and moisture feed ($r = 0.806$ and $r = 0.792$, $p < 0.05$, respectively). Consequently, all the extruded CS exhibited a significantly ($p < 0.05$) higher direct antioxidant capacity (22–77%) than the non-extruded one (110.5 mg TE/g). The CS extruded at 160 °C and 25% feed moisture showed the greatest rise in the AC (195.1 mg TE/g), and the one extruded at 135 °C and 15% feed moisture exhibited the lowest AC (134.9 mg TE/g) (Table 3). As previously reported in other food matrices, extrusion, primarily at high temperatures, enhanced the CS's antioxidant capacity (Benítez et al., 2021; Zhang et al., 2018).

Table 3

Impact of extrusion on the free, bound, and total phenolic compounds content and *in vitro* direct and indirect antioxidant capacity in the cocoa shell under different temperature (135–150 or 160–175 °C) and moisture (15, 20, or 25%) processing conditions. Release of phenolic compounds and remaining phenolic content in the insoluble non-digested residue in the gastric and intestinal phases of the simulated digestion and corresponding antioxidant capacity of the remaining and released compounds in gastric and intestinal phases.

	Total Phenolic Compounds (mg/GAE g)				Bioaccessibility (%)		Antioxidant Capacity (mg/TE g)					Recovery (%)	
	Free	Bound	Total	Released	Free†	Total‡	Free	Bound	Total	Direct	Released	Free	Total
Raw	<i>FPC</i>	<i>BPC</i>	<i>TPC</i>				<i>AC-FPC</i>	<i>AC-BPC</i>	<i>AC-TPC</i>	<i>Direct AC</i>			
Control	18.8 ± 1.1 ^a	10.2 ± 0.9 ^c	28.9 ± 1.2 ^{ab}	–	–	–	22.7 ± 1.3 ^{bc}	11.7 ± 0.7 ^b	34.4 ± 1.6 ^b	110.5 ± 4.8 ^a	–	–	–
E135–15	18.0 ± 0.8 ^a	5.1 ± 0.3 ^{ab}	23.1 ± 0.6 ^a	–	–	–	20.1 ± 0.6 ^a	6.7 ± 0.8 ^a	26.8 ± 1.2 ^a	134.9 ± 10.0 ^b	–	–	–
E135–20	19.0 ± 1.9 ^a	7.9 ± 0.6 ^{bc}	26.8 ± 2.3 ^{ab}	–	–	–	20.9 ± 0.6 ^{ab}	12.0 ± 0.7 ^b	33.0 ± 1.3 ^b	158.0 ± 4.5 ^c	–	–	–
E135–25	18.7 ± 1.2 ^a	13.5 ± 2.2 ^d	32.2 ± 3.2 ^{bc}	–	–	–	22.5 ± 0.8 ^{bc}	15.1 ± 1.6 ^b	37.6 ± 1.9 ^c	161.0 ± 13.5 ^c	–	–	–
E160–15	20.4 ± 3.6 ^a	4.1 ± 1.0 ^a	24.6 ± 3.6 ^a	–	–	–	23.0 ± 0.9 ^c	6.3 ± 0.8 ^a	29.3 ± 1.5 ^a	162.6 ± 7.1 ^c	–	–	–
E160–20	21.1 ± 2.6 ^a	8.2 ± 0.8 ^{bc}	29.3 ± 2.7 ^{ab}	–	–	–	23.3 ± 2.5 ^c	12.1 ± 1.2 ^b	35.4 ± 1.1 ^{bc}	169.4 ± 12.7 ^c	–	–	–
E160–25	29.6 ± 1.4 ^b	7.1 ± 1.1 ^{abc}	36.7 ± 2.1 ^c	–	–	–	25.6 ± 2.4 ^c	12.1 ± 1.6 ^c	37.7 ± 3.0 ^c	195.1 ± 5.3 ^d	–	–	–
Gastric Phase	<i>FPC-NDG</i>	<i>BPC-NDG</i>	<i>TPC-NDG</i>	<i>RPC-G</i>			<i>AC-FPC-NDG</i>	<i>AC-BPC-NDG</i>	<i>AC-TPC-NDG</i>		<i>AC-RPC-G</i>		
Control	19.1 ± 1.1 ^d	4.4 ± 0.9 ^a	23.5 ± 1.6 ^b	7.5 ± 1.9 ^a	–	–	22.8 ± 0.7 ^d	4.9 ± 1.2 ^a	27.7 ± 1.9 ^a	–	8.6 ± 0.4 ^a	–	–
E135–15	12.9 ± 1.0 ^a	10.4 ± 1.1 ^c	23.3 ± 0.8 ^b	8.7 ± 0.5 ^{ab}	–	–	12.5 ± 1.3 ^a	13.7 ± 0.7 ^d	26.2 ± 0.8 ^a	–	10.3 ± 0.4 ^b	–	–
E135–20	15.2 ± 1.4 ^{abc}	7.8 ± 0.6 ^b	22.2 ± 2.1 ^{ab}	8.0 ± 0.5 ^{ab}	–	–	17.9 ± 1.4 ^b	8.7 ± 1.5 ^b	26.5 ± 1.2 ^a	–	9.9 ± 0.3 ^b	–	–
E135–25	15.8 ± 1.3 ^{bc}	7.3 ± 2.1 ^b	23.2 ± 1.6 ^b	7.8 ± 0.5 ^{ab}	–	–	20.7 ± 0.9 ^{cd}	7.8 ± 1.6 ^b	28.5 ± 2.4 ^a	–	11.4 ± 0.1 ^c	–	–
E160–15	12.5 ± 1.0 ^a	7.5 ± 1.2 ^b	20.0 ± 1.5 ^a	9.3 ± 0.4 ^{bc}	–	–	17.5 ± 0.9 ^b	11.1 ± 0.9 ^c	28.6 ± 1.5 ^a	–	11.1 ± 0.3 ^c	–	–
E160–20	13.1 ± 0.9 ^{ab}	6.7 ± 1.2 ^{ab}	19.8 ± 1.4 ^a	10.5 ± 0.8 ^{cd}	–	–	19.4 ± 1.2 ^{bc}	8.7 ± 0.9 ^b	28.0 ± 2.0 ^a	–	11.1 ± 0.2 ^c	–	–
E160–25	17.1 ± 2.4 ^{cd}	5.3 ± 1.3 ^{ab}	22.4 ± 2.9 ^{ab}	11.9 ± 0.5 ^d	–	–	22.0 ± 0.9 ^d	7.0 ± 1.1 ^{ab}	29.0 ± 1.6 ^a	–	13.0 ± 0.6 ^d	–	–
Intestinal Phase	<i>FPC-NDI</i>	<i>BPC-NDI</i>	<i>TPC-NDI</i>	<i>RPC-I</i>			<i>AC-FPC-NDI</i>	<i>AC-BPC-NDI</i>	<i>AC-TPC-NDI</i>		<i>AC-RPC-I</i>		
Control	9.2 ± 0.5 ^{bc}	5.6 ± 0.5 ^b	14.8 ± 0.7 ^b	13.6 ± 0.4 ^a	73 ± 2 ^b	47 ± 1 ^{ab}	16.7 ± 1.6 ^a	12.4 ± 2.1 ^c	29.1 ± 3.6 ^b	–	23.1 ± 2.3 ^{ab}	102 ± 4 ^a	67 ± 3 ^{ab}
E135–15	7.7 ± 0.5 ^{abc}	5.3 ± 1.0 ^{ab}	13.0 ± 1.0 ^b	15.2 ± 0.4 ^{ab}	85 ± 2 ^c	66 ± 2 ^d	15.0 ± 2.4 ^a	12.1 ± 0.9 ^c	27.2 ± 2.3 ^b	–	24.3 ± 1.0 ^{abc}	121 ± 2 ^b	91 ± 1 ^d
E135–20	8.0 ± 0.3 ^{abc}	4.5 ± 0.6 ^{ab}	12.4 ± 0.8 ^{ab}	14.6 ± 0.4 ^{ab}	77 ± 2 ^{bc}	54 ± 2 ^c	15.0 ± 1.4 ^a	10.7 ± 1.1 ^{bc}	25.7 ± 0.6 ^b	–	23.5 ± 1.4 ^{ab}	112 ± 3 ^{ab}	71 ± 2 ^{ab}
E135–25	7.9 ± 0.4 ^{abc}	4.1 ± 0.4 ^{ab}	12.0 ± 0.3 ^{ab}	14.1 ± 0.3 ^a	75 ± 2 ^{bc}	44 ± 1 ^a	15.1 ± 1.7 ^a	11.4 ± 1.7 ^c	26.5 ± 0.9 ^b	–	22.2 ± 1.7 ^a	99 ± 3 ^a	59 ± 2 ^a
E160–15	6.4 ± 0.6 ^a	1.8 ± 0.4 ^a	8.2 ± 0.7 ^a	15.7 ± 0.5 ^{ab}	77 ± 2 ^{bc}	64 ± 2 ^d	13.8 ± 1.5 ^a	6.6 ± 0.9 ^a	20.5 ± 1.2 ^a	–	25.5 ± 2.9 ^{abc}	111 ± 7 ^{ab}	87 ± 5 ^{cd}
E160–20	6.8 ± 0.8 ^{ab}	4.3 ± 0.6 ^{ab}	11.1 ± 0.9 ^{ab}	16.7 ± 0.8 ^{bc}	74 ± 2 ^b	53 ± 1 ^{bc}	15.7 ± 0.9 ^a	10.1 ± 1.3 ^{bc}	25.8 ± 1.2 ^b	–	26.5 ± 1.7 ^{bc}	114 ± 3 ^{ab}	75 ± 2 ^{bc}
E160–25	10.2 ± 0.6 ^c	3.1 ± 1.2 ^{ab}	13.3 ± 1.5 ^b	18.1 ± 0.4 ^c	61 ± 1 ^a	49 ± 1 ^{abc}	19.1 ± 1.8 ^b	8.1 ± 0.8 ^{ab}	27.2 ± 1.6 ^b	–	28.9 ± 2.1 ^c	113 ± 3 ^{ab}	77 ± 2 ^{bc}

The results are reported as mean ± SD ($n = 3$). Mean values within the same column followed by different letters significantly ($p < 0.05$) differ according to ANOVA and Tukey's multiple range test. FPC: Free Phenolic Compounds; BPC: Bound Phenolic Compounds; TPC: Total Phenolic Compounds; AC: Antioxidant Capacity; RPC: Released Phenolic Compounds; G: Gastric; I: Gastrointestinal; NDG: Non-Digested Gastric; NDI: Non-Digested Gastrointestinal; †PC-Bioaccessibility-F: Phenolic Compounds Bioaccessibility related to Free phenolics; ‡PC-Bioaccessibility-T: Phenolic Compounds Bioaccessibility related to Total Phenolics.

3.4. High-temperature and high-moisture extrusion increased phenolic compounds release, but low-moisture extrusion improved their bioaccessibility

Although the chemical extraction provides insight into phenolic compounds potentially released in the small intestine during gastrointestinal digestion (FPC) and in the colon after microbial metabolism (BPC) (Cañas et al., 2022), simulated gastrointestinal digestion better reflects the behavior of phenolic compounds under physiological conditions (Brodtkorb et al., 2019). Extrusion at a high temperature (160 °C) significantly ($p < 0.05$) favored the release of phenolic compounds (RPC) during simulated gastrointestinal conditions at both gastric

(24–58%) and intestinal (14–33%) phases compared to the non-extruded CS, promoting the phenolic's release at the highest (25%) moisture feed (Table 3). Significant RPC increases were accompanied by a lower concentration of total phenolic compounds in the insoluble non-digested residue of the gastric phase (TPC-NDG). In addition, the gastric digestion media of extruded samples exhibited a higher *in vitro* antioxidant capacity (AC-RPC-G) than the non-extruded CS, i.e., 15–32% (135 °C) and 29–33% (160 °C) (Table 3). The AC-RPC-G was correlated with both extrusion temperature and moisture parameters ($r = 0.890$ and $r = 0.863$, $p < 0.05$, respectively). Nevertheless, the antioxidant capacity of the total phenolic compounds extracted from the non-digested gastric residue (AC-TPC-NDG) seemed not to be affected by

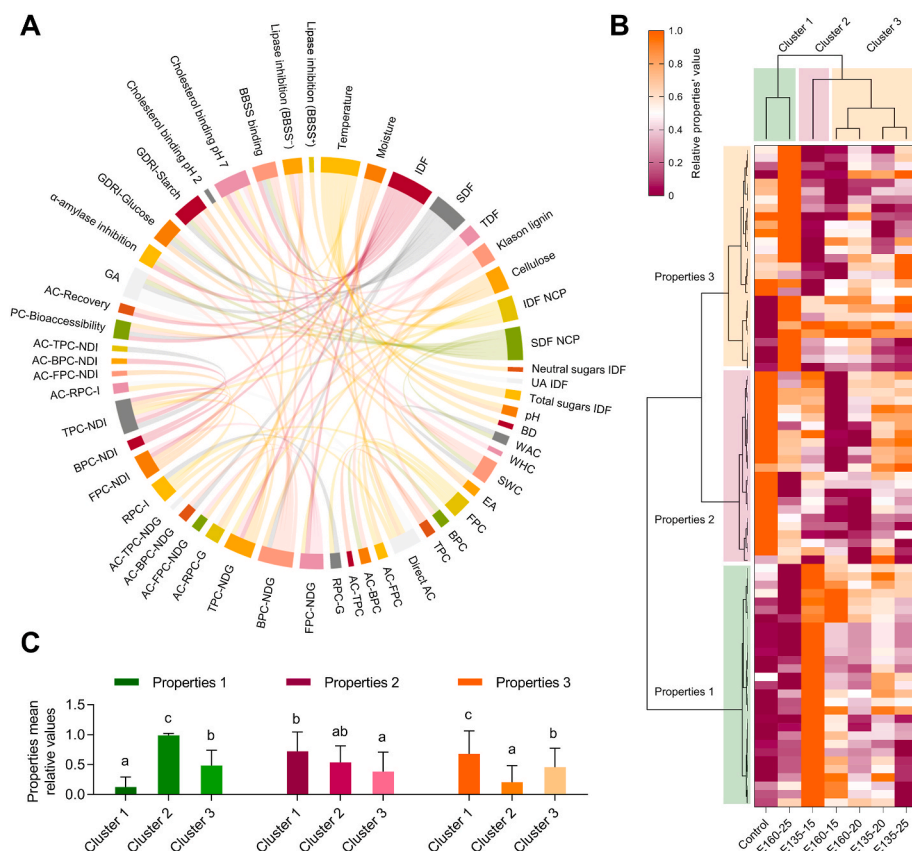


Fig. 2. Chord diagram illustrating the significant ($p < 0.05$) Pearson correlations among the extrusion parameters for the cocoa shell, dietary fiber and phenolics' composition, physicochemical and techno-functional properties, and *in vitro* physiological properties (A). Agglomerative hierarchical cluster analysis coupled to heat map (from the lowest (■) to the highest (■) relative value for each parameter) (B) showing the associations among the measured properties and classifying extruded cocoa shell samples according to them. Average relative values for each property set (1–3) in each sample cluster (1–3) (C). Bars with different letters significantly ($p < 0.05$) differ according to ANOVA and Tukey's multiple range test. IDF: Insoluble Dietary Fiber; SDF: Soluble Dietary Fiber; NCP: Non-Cellulosic Polysaccharides; UA: Uronic Acids; BD: Bulk Density; WAC: Water absorption Capacity; WHC: Water Holding Capacity; SWC: Swelling Capacity; EA: Emulsifying Activity; FPC: Free Phenolic Compounds; BPC: Bound Phenolic Compounds; TPC: Total Phenolic Compounds; AC: Antioxidant Capacity; RPC: Released Phenolic Compounds G: Gastric; I: Gastrointestinal; NDG: Non-Digested Gastric; NDI: Non-Digested Gastrointestinal; PC-Bioaccessibility: Phenolic Compounds Bioaccessibility; GA: Glucose Adsorption; GDRI: Glucose Diffusion Retardation Index; BBSS: Bile Salts.

extrusion.

The antioxidant capacity in the intestinal phase (AC-RPC-I) significantly increased at high temperatures (160 °C) and high moisture (25%) (Table 3). The mentioned antioxidant capacity was closely associated with the content of phenolic compounds released in the intestinal media (RCP-I) ($r = 0.950$, $p < 0.05$) and with FPC ($r = 0.878$, $p < 0.05$). A significant decrease in the antioxidant capacity from the total phenolic extracted from the insoluble non-digested intestinal residue (AC-TPC-NDI) was observed at 160 °C–15% moisture extrusion conditions due to the loss of total phenolics (TPC-NDI) ($r = 0.969$, $p < 0.05$). Cañas et al. (2022) demonstrated that the main phenolic compounds released from the CS during gastrointestinal digestion include catechin and gallic and protocatechuic acids. We previously found that those phenolic compounds are tightly bound to the dietary fiber matrix (BPC) but highly associated with the CS antioxidant properties (Rebollo-Hernanz et al., 2021; Cañas et al., 2023). Therefore, we foresee that extrusion might liberate those compounds from the dietary fiber matrix, allowing their enhanced release during gastrointestinal digestion.

Milder extrusion conditions (135 °C–15% moisture) significantly improved the bioaccessibility of phenolic compounds (PC-Bioaccessibility) relative to FPC and TPC (PC-Bioaccessibility-F and PC-Bioaccessibility-T) (17% and 40%, respectively) (Table 3). In addition, the recovered antioxidant capacity in the extruded CS was higher than in the non-extruded CS, i.e., 19% and 35% relative to FPC-AC and TPC-AC, respectively, at 135 °C–15%, and 30% regarding TPC-AC at 160 °C–15% (Table 3). The antioxidant capacity recovery index was associated with PC-Bioaccessibility-T ($r = 0.939$, $p < 0.05$). The improved bioaccessibility might be due to the decrease of the binding between phenolic compounds and cell walls components, triggered by the degradation of the IDF polysaccharides (cellulose and hemicellulose) and lignin during extrusion (Herrera-Cazares et al., 2021). Accordingly,

we observed an inverse correlation ($p < 0.05$) between PC-Bioaccessibilities and the content of glucose in IDF ($r = -0.842$), cellulose ($r = -0.798$), and lignin ($r = -0.808$). Our findings suggest that extrusion cooking could be viewed as a strategy for promoting the solubilization of phenolic compounds bound to the CS dietary fiber matrix. Research has previously shown that bound phenolics, primarily linked to cell wall components, are connected to the dietary fiber matrix through hydrophobic interactions, hydrogen bonds (between phenolic acids' hydroxyl group and the oxygen atoms of glycosidic linkages in hemicelluloses sugar residues), and covalent bonds (ester bonds between phenolic acids carboxy group and polysaccharides' hydroxyl group, or ether linkages between hydroxyl groups of phenolics and lignins) (Liu et al., 2020). Correspondingly, glycosidic/ester/ether bonds in hemicelluloses, celluloses, and lignin may be hydrolyzed during the extrusion process (Giummarella et al., 2019).

3.5. Extrusion modified the techno-functional properties of the cocoa shell

The extruded CS exhibited similar pHs to the non-extruded CS (Table 4). The pH is associated with other techno-functional properties, mainly those related to proteins, such as emulsifying activity (EA). Then, the absence of pH changes might explain the invariable EA of the extruded CS after extrusion (Table 4). All the studied extrusion treatments showed a significant ($p < 0.05$) increase in BD, as previously supported by Wang et al. (2022). The bulk density (BD) is an essential parameter in extruded food production closely tied to the expansion capacity (Oladiran and Emmambux, 2018). Consequently, Jozinović et al. (2019) observed a decreasing expansion ratio of corn: CS extrudates when increasing the proportion of the CS. In general, the extrusion process significantly ($p < 0.05$) decreased the ability of the CS to hold oil (22–28%) from 1.8 mL/g in the non-extruded CS to 1.3–1.4 mL/g in the

Table 4

Effect of extrusion on the physicochemical and techno-functional properties of the cocoa shell (CS) under processing conditions of 135–150 or 160–175 °C and 15, 20, or 25% moisture.

	pH	EA (%)	BD (g/mL)	OHC (mL/g)	WAC (mL/g)	WHC (mL/g)	SWC (mL/g)
Control	5.8 ± 0.2 ^a	15.1 ± 1.5 ^a	0.48 ± 0.00 ^a	1.8 ± 0.2 ^b	2.8 ± 0.2 ^b	3.4 ± 0.0 ^d	7.0 ± 0.0 ^b
E135–15	5.6 ± 0.1 ^a	15.3 ± 2.1 ^a	0.65 ± 0.00 ^b	1.3 ± 0.1 ^a	3.6 ± 0.2 ^c	2.8 ± 0.0 ^c	9.5 ± 0.5 ^d
E135–20	5.5 ± 0.1 ^a	17.8 ± 1.8 ^a	0.64 ± 0.00 ^b	1.4 ± 0.0 ^a	3.3 ± 0.3 ^c	2.8 ± 0.0 ^c	9.3 ± 0.0 ^d
E135–25	5.5 ± 0.1 ^a	17.5 ± 1.6 ^a	0.61 ± 0.00 ^b	1.4 ± 0.1 ^a	3.0 ± 0.3 ^{bc}	2.4 ± 0.0 ^c	8.0 ± 0.0 ^c
E160–15	5.5 ± 0.1 ^a	15.1 ± 1.5 ^a	0.64 ± 0.01 ^b	1.4 ± 0.1 ^a	2.6 ± 0.3 ^{ab}	2.2 ± 0.0 ^b	8.3 ± 0.0 ^c
E160–20	5.5 ± 0.2 ^a	17.8 ± 1.9 ^a	0.62 ± 0.02 ^b	1.6 ± 0.0 ^b	2.4 ± 0.2 ^a	2.0 ± 0.1 ^b	8.0 ± 0.3 ^c
E160–25	5.3 ± 0.1 ^a	18.1 ± 1.7 ^a	0.61 ± 0.01 ^b	1.4 ± 0.0 ^a	2.0 ± 0.2 ^a	1.2 ± 0.0 ^a	5.0 ± 0.5 ^a

Results are reported as mean ± SD ($n = 3$). Mean values within a column followed by different superscript letters are significantly different when subjected to Tukey's test ($p < 0.05$). BD: Bulk Density; WHC: Water Holding Capacity; WAC: Water Absorption Capacity; OHC: Oil Holding Capacity; SWC: Swelling Capacity; EA: Emulsifying Activity.

extruded ones. These results infer that extrusion may reduce the non-polar residues availability on the surface of the CS, probably due to the decreased particle size and hydrophobic groups in the extruded CS (Li et al., 2019).

The successful inclusion of fiber-enriched ingredients into foods can be influenced by their water-holding (WHC), water absorption (WAC), and swelling (SWC) capacities. The extruded CS exhibited significant ($p < 0.05$) lower WHC (18–65%) than the non-extruded one (3.4 mL/g), higher at 160 than at 135 °C, being maximum at 160 °C–25% moisture (1.2 mL/g) (Table 3). Hence, results supported that increasing extrusion temperature might reduce the WHC (Li et al., 2019). The reduction of galactose and arabinose observed in the IDF of the extruded CS correlated with the WHC ($r = 0.819$ and $r = 0.879$, $p < 0.05$, respectively). Losses in arabinose- and galactose-containing polysaccharides may diminish the water interaction sites of the extruded CS. Conversely, extrusion increased the WAC at 135 °C and decreased it at 160 °C, whereas barrel moisture feed did not affect this property. These findings could be associated with the modifications displayed by the extrusion process in the IDF and SDF content and composition. Results showed correlations ($p < 0.05$) between the WAC and the content of cellulose ($r = -0.831$), the SDF concentration ($r = 0.774$), and the SDF total neutral sugars content ($r = 0.837$) (Fig. 2A). Then, the reduction in the cellulose content, while the SDF content increased, resulted in improved WAC properties. Cellulose showed a similar WAC (2.8 mL/g), whereas pectin exhibited much higher values (9.9 mL/g) (Benítez et al., 2019). Moreover, the WAC correlated with the SWC ($r = 0.850$, $p < 0.05$). In this context, extrusion also increased significantly ($p < 0.05$) SWC (14–35%), except for the CS extruded at 160 °C–25% of moisture feed. As observed for the WAC, the SWC showed a larger increase at 135 °C and 15 or 20% of moisture feed due to their higher SDF content, which was supported by the correlation observed between the SWC and SDF polysaccharides ($r = 0.813$, $p < 0.05$). Extrusion yielded similar effects on coffee parchment; extrusion at low moisture increases the SWC (Benítez et al., 2021). The inclusion of the CS in an extruded food matrix would provide good hydration properties due to their high hydration

properties (Dey et al., 2021).

Based on our results, extrusion modified the techno-functional properties of the cocoa shell, producing a more compact CS with slightly less capacity to hold oil and water and slightly higher swelling properties. Then, the CS might be used to reduce the caloric content or modify the texture of extruded products. In addition, the mentioned modifications could imply changes in the extruded CS's physiological effects, such as their hypoglycemic and hypolipidemic capacities.

3.6. Extrusion enhanced *in vitro* hypoglycemic properties due to the higher proportion of soluble fiber in the extruded cocoa shell

The glucose adsorption capacity of the extruded CS depended on the glucose concentration (Fig. 3A). Extrusion (all conditions) significantly ($p < 0.05$) increased the CS's glucose adsorption capacity at 100 and 200 mM but not at low glucose concentrations (10–50 mM), highlighting the capacity to adsorb glucose of those samples extruded with 15 and 20% moisture feed. Extrusion at 135 °C–15% moisture showed the highest increase for glucose adsorption (2.2–2.9-fold, $p < 0.05$, depending on the glucose concentration in the medium) and the maximum glucose adsorbed per gram of sample (2.1-fold, $p < 0.05$), along with CS extruded at 135 °C–20% and 160 °C–15% (Fig. 3A and B). The extruded CS glucose adsorption capacity strongly correlated with their respective SDF content ($r = 0.965$, $p < 0.05$) (Fig. 2A). The increased contribution of SDF to TDF after extrusion may influence the higher glucose adsorption capacity of the extruded CS, as previously suggested by Garcia-Valle et al. (2021). These results may indicate that extrusion with 15 and 20% moisture feed could promote the ability of the CS to reduce the amount of glucose available in the intestinal lumen to a greater extent than the non-extruded CS and, consequently, attenuate the postprandial glucose increase.

The extruded CS exhibited a significantly ($p < 0.05$) higher capacity (29–54%) to inhibit the α -amylase activity compared to the non-extruded CS, except for the treatments with 25% moisture feed at both temperatures. However, no significant differences were found among the extrusion treatments at 15 and 20% moisture feed (Fig. 3C). The observed inhibition showed a strong correlation with SDF and IDF, being inversely proportional for the latest ($r = 0.888$ and $r = -0.911$, $p < 0.05$, respectively) (Fig. 2A). Therefore, the higher capacity exhibited could be explained by the IDF decrease and the increased SDF contribution noted in the extruded CS (Fig. 1A and B). The α -amylase inhibition displayed by the extruded CS could expand carbohydrates' digestion time and limit the glucose release from starch (Punia Bangar et al., 2022). Thus, reduced α -amylase activity may decrease the rate of glucose absorption and, consequently, diminish the postprandial plasma glucose.

The CS extruded at 135 °C (15–25% moisture) and 160 °C (15% moisture) showed a significantly lower ($p < 0.05$) dialyzed glucose (Fig. 3D) and V_{\max} (2.1–2.2 $\mu\text{mol}/\text{min}$) (Fig. 3E) compared to the non-extruded CS (2.7 $\mu\text{mol}/\text{min}$). Moreover, extrusion raised (73–91%, $p < 0.05$) the GDRI-glucose (Fig. 4F). The improvement of glucose diffusion retardation may be associated with the SDF content since GDRI-glucose and V_{\max} were directly and inversely associated, respectively, with this parameter ($r = 0.852$ and $r = -0.849$, $p < 0.05$) (Fig. 2A). Therefore, the higher SDF proportion promoted by extrusion increased the CS's ability to retard glucose diffusion. This capacity may be related to the physical impediment offered by fiber particles to glucose molecules due to the rheological properties of fiber polysaccharides, together with the CS' capacity to adsorb glucose ($r = 0.782$, $p < 0.05$) (Zhu et al., 2021).

Moreover, all the extruded CS flours significantly reduced ($p < 0.05$) starch hydrolysis in comparison to the non-extruded CS from 60 min onwards and exhibited increased GDRI-starch ($p < 0.05$) up to 2.8-fold in 135 °C–15% moisture compared to non-extruded CS (Control, 20%) (Fig. 3G, I). The CS extruded at 135 °C and 15–20% moisture feed, as well as that obtained at 160 °C and 15% moisture feed, showed a significantly lower V_{\max} (0.09 $\mu\text{mol}/\text{min}$, $p < 0.05$) compared to the

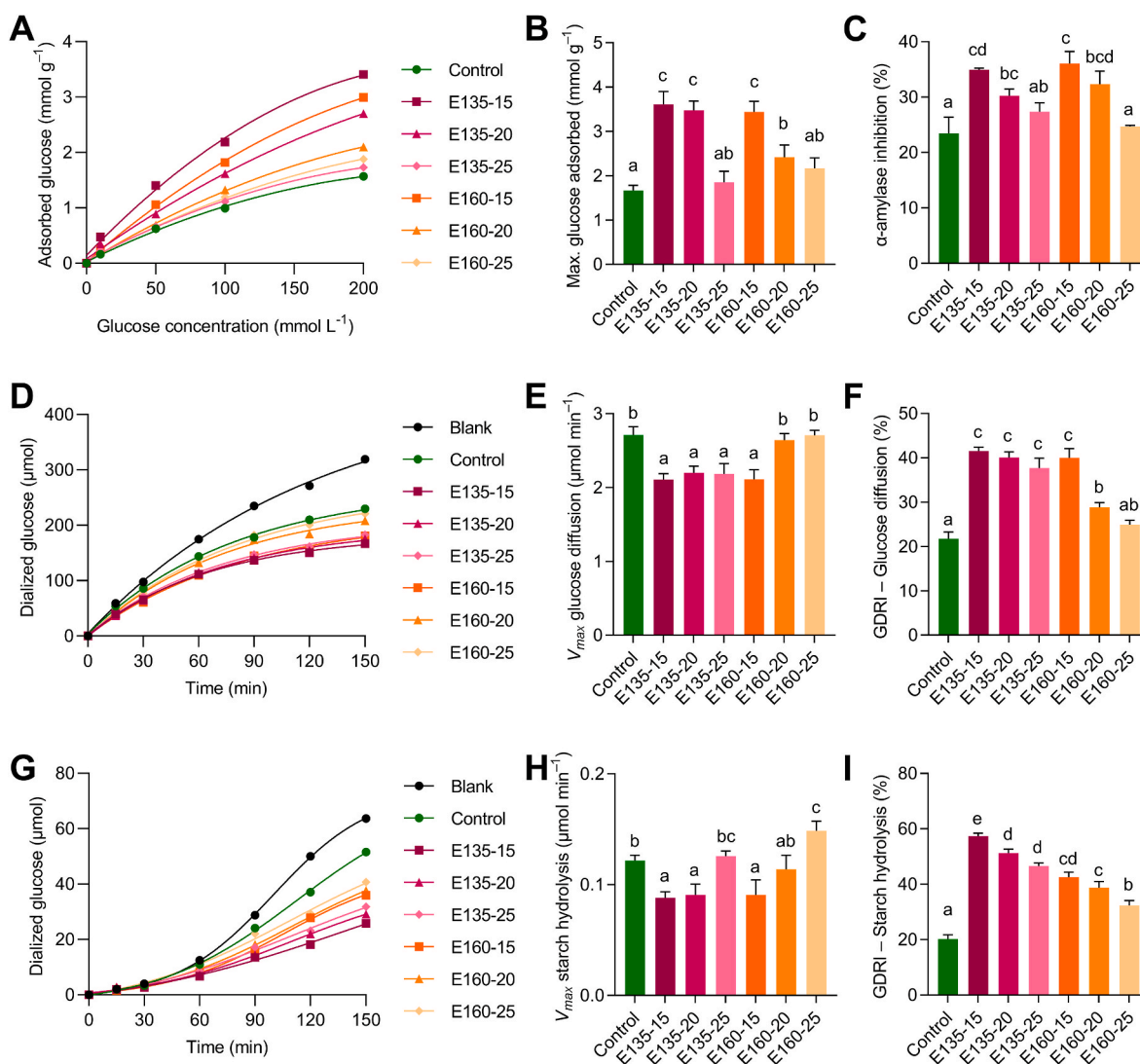


Fig. 3. Effect of extrusion on the cocoa shell's glucose adsorption capacity (A), maximum glucose adsorbed (mmol/g) (B), α -amylase inhibition (C), glucose diffusion kinetics (0–150 min) (D), V_{\max} glucose diffusion (E), glucose diffusion retardation index (GDRI) (F), starch hydrolysis kinetics (0–150 min) (G), V_{\max} (H) and GDRI (I) for glucose release from starch under different temperature (135–150 or 160–175 °C) and moisture (15, 20, or 25%) processing conditions. The results are reported as mean \pm SD ($n = 3$). Bars and points with different letters significantly ($p < 0.05$) differ according to ANOVA and Tukey's multiple range test.

non-extruded CS (0.12 $\mu\text{mol}/\text{min}$) (Fig. 3H). Therefore, results showed that extrusion enhanced the CS's capacity to reduce starch digestibility. This effect might be related to the SDF content and the other hypoglycemic properties since the GDRI-starch was correlated ($p < 0.05$) to the content of SDF ($r = 0.846$), the GDRI-glucose ($r = 0.925$), the glucose adsorption capacity ($r = 0.832$), and α -amylase inhibition ($r = 0.700$) (Fig. 2A). The modifications promoted by extrusion in the dietary fiber from the CS, especially regarding the SDF proportion, led to the higher ability of the extruded CS to retard starch digestibility. Interestingly, there were no associations between the concentration of phenolic compounds and the CS's hypoglycemic properties. Dietary fiber, phenolic compounds, and their interactive complexes have demonstrated glucose absorption delaying properties (Dobson et al., 2019; Taladrid et al., 2023). Nonetheless, the hypoglycemic properties of the extruded CS were mainly governed by dietary fiber. Hence, the improved hypoglycemic properties found in the extruded CS could probably be due to the SDF increase, which triggered a strengthened capacity to adsorb glucose, diminishing glucose diffusion and reducing the enzyme accessibility to starch as the polysaccharide entrapment or enzyme in the matrix.

3.7. Extrusion preserved the *in vitro* hypolipidemic properties of the cocoa shell

Results indicated that the cholesterol-binding capacity of the extruded CS depended on the pH of the media. In general terms, at pH 2, both the extruded and non-extruded CS showed a similar capacity to bind cholesterol (37–50%), except for the CS extruded at 160 °C–25% moisture, whose capacity to bind cholesterol increased significantly ($p < 0.05$) up to 66% (Fig. 4A). However, extrusion produced a significant decrease ($p < 0.05$) in the ability to bind cholesterol at pH 7, except for 135–25%, being significantly more pronounced at 160 °C (48–57%) than at 135 °C with 15 and 20% moisture feed (30 and 21%, respectively). The mentioned trend could be due to the reduction of the TDF content, specifically, the decrease of IDF, since, at pH 7, cholesterol binding notably correlated with TDF and IDF ($r = 0.872$ and $r = 0.810$, $p < 0.05$, respectively). This drop could be associated ($p < 0.05$) with the loss of non-cellulosic polysaccharides in IDF ($r = 0.896$), constituted by arabinose ($r = 0.913$), galactose ($r = 0.845$), and uronic acids ($r = 0.909$) (Fig. 2A). Therefore, it can be claimed that dietary fiber, IDF non-cellulosic polysaccharides in this specific case, can delay cholesterol absorption, although the involved mechanisms remain unclear. Some

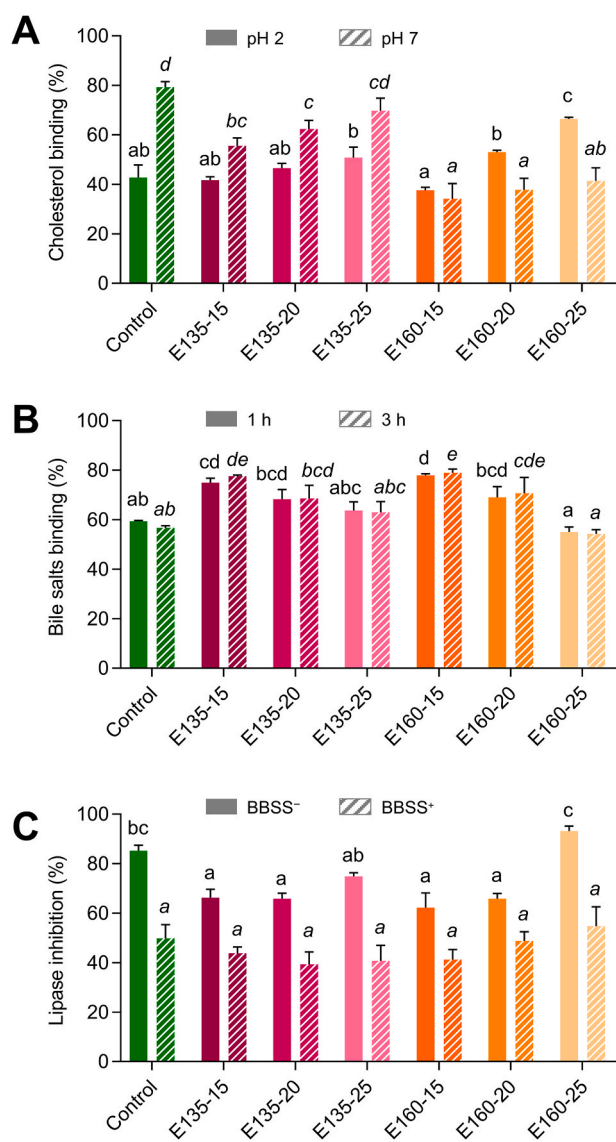


Fig. 4. Effect of extrusion on the cocoa shell's cholesterol-binding capacity (%) at pH 2 (solid bars) and pH 7 (striped bars) (A), bile salt binding capacity (%) after 1 h (solid bars) and 3 h (striped bars) of incubation (B), and *in vitro* lipase inhibition in a model without bile salts (BBSS⁻, solid bars) and with them (BBSS⁺, striped bars) (C) at several temperature (135–150 or 160–175 °C) and moisture (15, 20, or 25%) processing conditions. The results are reported as mean \pm SD ($n = 3$). Bars and points with different letters significantly ($p < 0.05$) differ according to ANOVA and Tukey's multiple range test.

authors proposed a direct binding of fiber to cholesterol in the intestinal lumen or a reduction of its emulsification by bile salts, delaying its diffusion to the intestinal epithelial cells (Acevedo-Fani and Singh, 2022). The extruded CS exhibited a similar or higher cholesterol binding capacity than other dietary fibers from food by-products, commercial citrus pectin, or even cholestyramine (Bagabaldo et al., 2022; Taladrid et al., 2023). Then, the extruded CS might be an attractive fiber-rich ingredient with hypocholesterolemic effects.

The extruded and non-extruded CS revealed noticeable bile salts' adsorption capacity, between 54 and 79% (Fig. 4B), not being affected by incubation time (1–3 h) ($p > 0.05$). The extruded CS bound from 23 to 35 mg of sodium cholate per gram. Only extrusion at 15% moisture feed at both temperatures significantly enhanced the CS capacity to bind bile salts (26–39%). This improvement could be significantly ($p < 0.05$) correlated to the decrease of IDF ($r = -0.852$) and the increase in the

proportion of SDF ($r = 0.801$) together with the changes produced by extrusion in its composition, particularly in the contents of mannose ($r = 0.920$), rhamnose ($r = 0.897$) and uronic acids ($r = 0.797$) (Fig. 2A). Therefore, these sugar residues may be responsible for the dietary fiber binding to bile salts. As previously reported, the reduction of bile salts availability in the small intestine, exhibited by the extruded CS, can inhibit its surfactant activity (Islam et al., 2022). Consequently, decreased micelles formation and hindered lipid digestion and absorption might reduce circulating triglycerides. In addition, the bile salt binding capacity of the extruded CS blocks their reabsorption, which may require the use of cholesterol in hepatocytes to preserve the bile salt reserve, thereby reducing plasma cholesterol levels (Islam et al., 2022).

The capacity of the extruded CS to inhibit pancreatic lipase was analyzed in the absence or presence of bile salts (BBSS⁻ and BBSS⁺, respectively) (Fig. 4C). In the BBSS⁻ model, extrusion at 15–20% moisture feed at both temperatures significantly reduced the CS's lipase inhibitory ability (22–27%, $p < 0.05$) compared to the non-extruded material, whereas, in the BBSS⁺ model, such property was preserved. The modifications produced by extrusion in the TPC might cause the mentioned decrease in lipase inhibition in the first model ($r = 0.805$, $p < 0.05$). Nevertheless, all the extruded CS flours displayed high inhibitory ability against pancreatic lipase (40–93%) (Fig. 4C). Lipase inhibition by the extruded CS could be associated with dietary fiber and phenolic compounds, as previously proposed (Liu et al., 2020). Whether phenolic compounds can interact with the catalytic site of pancreatic lipase, dietary fiber could form a coating around lipid droplets, hindering lipase access to fat globules, decreasing lipid accessibility, trapping the enzyme within its matrix, or sequestering calcium ions necessary for enzyme activity (Acevedo-Fani and Singh, 2022). Due to their ability to inhibit lipase activity, adsorb cholesterol, and bind bile salts, the extruded CS could be an ingredient with promising hypolipidemic properties.

3.8. Extrusion modified the cocoa shell dietary fiber and phenolic compounds determining differential functional and physiological properties

Hierarchical clustering coupled with a heatmap (Fig. 3B) classified samples into three groups. The first group clustered the non-extruded CS and the CS extruded at 160 °C and 25% moisture. The second group was composed of extruded CS at low temperature and low moisture (135 °C and 15%), and the third group included the remaining samples (CS extruded at 160 °C, 15 and 20% moisture, and at 135 °C, 20 and 25% moisture feed). Similarly, the extruded CS's properties were clustered in three groups. The second group of samples (Cluster 2) was characterized by high values in the first set of properties (Properties 1, including SDF, phenolics bioaccessibility, WAC, hypoglycemic properties, and bile salts binding), followed by clusters 3 and 1 (Fig. 3C). The second set of properties was similar among clusters and included IDF, pH, WHC, and phenolics bound to insoluble non-digestible residues. Finally, the last set of properties, characterized by low values in cluster 2, and higher in clusters 1 and 3, included mainly phenolic compounds (free, bound, and released) and their antioxidant capacity, and cholesterol binding and lipase inhibition properties. Accordingly, extrusion produced two differential effects: solubilization of dietary fiber at 135 °C and low moisture (15%), correlated with higher hypoglycemic properties, or an increase in phenolic compounds and antioxidant capacity at 160 °C and high moisture (25%) associated with higher lipase inhibition. The other middle extrusion conditions combinations (cluster 3) yielded intermediate effects. Then, extrusion of the CS modified the content and profile of dietary fiber and phenolic compounds, determining differential functional and physiological properties.

Current research focuses on the incorporation of food by-products as ingredients into extruded products. This approach seeks the dual goal of valorizing residues while improving the nutritional quality of extruded foods (Santos et al., 2022). In this sense, we have demonstrated that the cocoa shell could be effectively extruded, providing attractive chemical and techno-functional traits to the added products. The solubilization of

dietary fiber during the extrusion of the CS may yield food ingredients with improved dietary fiber content and profile. Within the array of innovative techniques presently used for this purpose (mechanical, chemical, or enzymatic hydrolysis; microbiological fermentation, and thermal processes), extrusion cooking has been highlighted as one of the best options for disrupting the covalent and non-covalent interactions within cell wall polysaccharides and modifying the insoluble dietary fiber into smaller and more soluble molecular fragments (Bader Ul Ain et al., 2019). Considering the complex structure of the CS dietary fiber, comprising strong phenolic-polysaccharide interactions, extrusion was proven to be an effective technique for promoting phenolic compounds solubilization. Bound phenolic compounds and phenolic-dietary fiber interactions possess meaningful implications related to the bioaccessibility of phenolic compounds and, therefore, on the biological activity that those may exert in the organism (Rocchetti et al., 2022; Taladrí et al., 2023). The CS dietary fiber matrix protects phenolic compounds during gastrointestinal digestion but also hinders their final release in the gut due to such intense interactions (Cañas et al., 2022). Notwithstanding, the CS antioxidant fiber-phenolic complexes may entail significant reciprocal effects on the gut microbiota. Extrusion might promote fiber and phenolic compounds' colonic biotransformation, yielding exciting biological effects (Rocchetti et al., 2022; Taladrí et al., 2023). Ultimately, extrusion may serve as a strategy for utilizing the CS as an ingredient and improving extruded products' physiological and health-related effects while modifying their chemical and functional properties (Yi et al., 2022).

4. Conclusion

Extrusion of the CS decreased the total dietary fiber at 160 °C, while it did not change at 135 °C due to the IDF's solubilization, which increased the SDF. In addition, the extruded CS dietary fiber exhibited a better SDF: IDF ratio because of the higher contribution of the SDF fraction. Extrusion at high temperatures and high moisture feed (160 °C–25%) yielded a higher antioxidant capacity and phenolic compounds content, but the milder extrusion conditions (135 °C–15%) significantly enhanced the *in vitro* bioaccessibility of these bioactive compounds. Changes in the composition and structure of the extruded CS flours impacted the techno-functional properties, generating compact flours with slightly less capacity to hold oil and water and higher swelling properties. Likewise, the fiber composition modifications produced in the extruded CS improved the *in vitro* hypoglycemic properties, whereas the *in vitro* hypolipidemic properties were maintained. This study revealed the feasibility of the CS to improve the nutritional value of extruded foods. However, further post-inclusion studies are needed to verify its effect in specific matrices.

Funding

This research was funded by the COCARDIOLAC project from the Spanish Ministry of Science and Innovation (RTI 2018-097504-B-I00) and the Excellence Line for University Teaching Staff within the Multi-annual Agreement between the Community of Madrid and the UAM (2019–2023). M. Rebollo-Hernanz, thanks the Ministry of Universities for his FPU contract (FPU15/04238) and for his grant for the requalification of the Spanish university system (CA1/RSUE/2021–00656).

CRedit authorship contribution statement

Vanessa Benítez: Conceptualization, Formal analysis, Investigation, Methodology, Supervision, Writing – original draft, Writing – review & editing. **Miguel Rebollo-Hernanz:** Conceptualization, Formal analysis, Investigation, Methodology, Visualization, Writing – original draft, Writing – review & editing. **Cheyenne Braojos:** Investigation, Methodology, Writing – review & editing. **Silvia Cañas:** Investigation, Methodology, Writing – review & editing. **Alicia Gil-Ramírez:** Writing –

review & editing. **Yolanda Aguilera:** Writing – review & editing. **María A. Martín-Cabrejas:** Conceptualization, Funding acquisition, Project administration, Supervision, Writing – original draft, Writing – review & editing.

Declaration of competing interest

The authors declare that there is no financial/personal interest or belief that could affect their objectivity.

Data availability

Data will be made available on request.

Acknowledgments

The authors thank Dr. V. Sanchis from the Department of Food Technology at the University of Lleida for providing the extrusion equipment. We thank the helpful assistance of Irene Aparicio and Maria Paz Villalba during sample preparation and analysis.

References

- Acevedo-Fani, A., Singh, H., 2022. Biophysical insights into modulating lipid digestion in food emulsions. *Prog. Lipid Res.* <https://doi.org/10.1016/j.plipres.2021.101129>.
- Bader Ul Ain, H., Saeed, F., Ahmed, A., Asif Khan, M., Niaz, B., Tufail, T., 2019. Improving the physicochemical properties of partially enhanced soluble dietary fiber through innovative techniques: a coherent review. *J. Food Process. Preserv.* 43, e13917 <https://doi.org/10.1111/jfpp.13917>.
- Bagabaldo, P.A.A., Atienza, L.M., Castillo-Israel, K.A.T., Estacio, M.A.C., Gaban, P.J.V., Maniawang, J.R.C., Gapasin, R.P., Estrillillo, A.G.M., Cena-Navarro, R.B., 2022. 'Saba' banana (*Musa acuminata* x *balbiana* BBB Group) peel pectin supplementation improves biomarkers of obesity and associated blood lipid disorders in obese hypercholesterolemic mice. *Curr. Res. Food Sci.* 5, 251–260. <https://doi.org/10.1016/j.crf.2022.01.016>.
- Belwal, T., Cravotto, C., Ramola, S., Thakur, M., Chemat, F., Cravotto, G., 2022. Bioactive compounds from cocoa husk: extraction, analysis and applications in food production chain. *Foods* 11 (798 11), 798. <https://doi.org/10.3390/foods11060798>, 2022.
- Benítez, V., Rebollo-Hernanz, M., Aguilera, Y., Bejerano, S., Cañas, S., Martín-Cabrejas, M.A., 2021. Extruded coffee parchment shows enhanced antioxidant, hypoglycaemic, and hypolipidemic properties by releasing phenolic compounds from the fibre matrix. *Food Funct.* 12, 1097–1110. <https://doi.org/10.1039/d0fo02295k>.
- Benítez, V., Rebollo-Hernanz, M., Hernanz, S., Chantres, S., Aguilera, Y., Martín-Cabrejas, M.A., 2019. Coffee parchment as a new dietary fiber ingredient: functional and physiological characterization. *Food Res. Int.* 122, 105–113. <https://doi.org/10.1016/j.foodres.2019.04.002>.
- Boeckx, P., Batters, M., Dewettinck, K., 2020. Poverty and climate change challenges for sustainable intensification of cocoa systems. *Curr. Opin. Environ. Sustain.* 47, 106–111. <https://doi.org/10.1016/j.cosust.2020.10.012>.
- Brodtkorb, A., Egger, L., Alvinger, M., Alvito, P., Assunção, R., Ballance, S., Bohn, T., Bourlieu-Lacanal, C., Boutrou, R., Carrière, F., Clemente, A., Corredig, M., Dupont, D., Dufour, C., Edwards, C., Golding, M., Karakaya, S., Kirkhus, B., Le Feunteun, S., Lesmes, U., Macierzanka, A., Mackie, A.R., Martins, C., Marze, S., McClements, D.J., Ménard, O., Minekus, M., Portmann, R., Santos, C.N., Soucho, I., Singh, R.P., Vegarud, G.E., Wickham, M.S.J., Weitschies, W., Recio, I., 2019. INFOGEST static *in vitro* simulation of gastrointestinal food digestion. *Nat. Protoc.* 14, 991–1014. <https://doi.org/10.1038/s41596-018-0119-1>.
- Cañas, S., Rebollo-Hernanz, M., Bermúdez-Gómez, P., Rodríguez-Rodríguez, P., Braojos, C., Gil-Ramírez, A., Benítez, V., Aguilera, Y., Martín-Cabrejas, M.A., 2023. Radical scavenging and cellular antioxidant activity of the cocoa shell phenolic compounds after simulated digestion. *Antioxidants* 12 (5), 1007. <https://doi.org/10.3390/antiox12051007>.
- Cañas, S., Rebollo-Hernanz, M., Braojos, C., Benítez, V., Ferreras-Charro, R., Dueñas, M., Aguilera, Y., Martín-Cabrejas, M.A., 2022. Gastrointestinal fate of phenolic compounds and amino derivatives from the cocoa shell: an *in vitro* and *in silico* approach. *Food Res. Int.* 121217 <https://doi.org/10.1016/j.foodres.2022.121217>.
- Dey, D., Richter, J.K., Ek, P., Gu, B.J., Ganjyal, G.M., 2021. Utilization of food processing by-products in extrusion processing: a review. *Front. Sustain. Food Syst.* 4, 304. <https://doi.org/10.3389/fsufs.2020.603751>.
- Dobson, C.C., Mottawea, W., Rodrigue, A., Buzati Pereira, B.L., Hammami, R., Power, K.A., Bordenave, N., 2019. Impact of molecular interactions with phenolic compounds on food polysaccharides functionality. In: *Advances in Food and Nutrition Research*. Academic Press, pp. 135–181. <https://doi.org/10.1016/bs.afnr.2019.02.010>.
- Espinosa-Ramírez, J., Rodríguez, A., De la Rosa-Millán, J., Heredia-Olea, E., Pérez-Carrillo, E., Serna-Saldivar, S.O., 2021. Shear-induced enhancement of technofunctional properties of whole grain flours through extrusion. *Food Hydrocolloids* 111, 106400. <https://doi.org/10.1016/j.foodhyd.2020.106400>.

- García-Valle, D.E., Agama-Acevedo, E., Nuñez-Santiago, M., del, C., Alvarez-Ramirez, J., Bello-Pérez, L.A., 2021. Extrusion pregelatinization improves texture, viscoelasticity and *in vitro* starch digestibility of mango and amaranth flours. *J. Funct. Foods* 80, 104441. <https://doi.org/10.1016/j.jff.2021.104441>.
- García-Amezquita, L.E., Tejada-Ortigoza, V., Pérez-Carrillo, E., Serna-Saldívar, S.O., Campanella, O.H., Welti-Chanes, J., 2019. Functional and compositional changes of orange peel fiber thermally-treated in a twin extruder. *Lebensm. Wiss. Technol.* 111, 673–681. <https://doi.org/10.1016/j.LWT.2019.05.082>.
- Giummarella, N., Pu, Y., Ragauskas, A.J., Lawoko, M., 2019. A critical review on the analysis of lignin carbohydrate bonds. *Green Chem.* 21, 1573–1595. <https://doi.org/10.1039/c8gc03606c>.
- Grasso, S., 2020. Extruded snacks from industrial by-products: a review. *Trends Food Sci. Technol.* 99, 284–294. <https://doi.org/10.1016/j.tifs.2020.03.012>.
- Herrera-Cazares, L.A., Luzardo-Ocampo, I., Ramírez-Jiménez, A.K., Gutiérrez-Urbe, J.A., Campos-Vega, R., Gaytán-Martínez, M., 2021. Influence of extrusion process on the release of phenolic compounds from mango (*Mangifera indica* L.) bagasse-added confections and evaluation of their bioaccessibility, intestinal permeability, and antioxidant capacity. *Food Res. Int.* 148 <https://doi.org/10.1016/j.foodres.2021.110591>.
- Islam, M.S., Sharif, A., Kwan, N., Tam, K.C., 2022. Bile acid sequestrants for hypercholesterolemia treatment using sustainable biopolymers: Recent advances and future perspectives. *Mol. Pharm.* <https://doi.org/10.1021/acs.molpharmaceut.2c00007>.
- Jozinović, A., Panak Balentić, J., Ackar, D., Babić, J., Pajin, B., Miličević, B., Guberac, S., Vrdoljak, A., Subarić, D., 2019. Cocoa husk application in the enrichment of extruded snack products. *J. Food Process. Preserv.* 43 <https://doi.org/10.1111/jfpp.13866>.
- Kumar, V., Sharma, N., Umesh, M., Selvaraj, M., Al-Shehri, B.M., Chakraborty, P., Duhan, L., Sharma, S., Pasirja, R., Awasthi, M.K., Lakkaboyana, S.R., Andler, R., Bhatnagar, A., Maitra, S.S., 2022. Emerging challenges for the agro-industrial food waste utilization: a review on food waste biorefinery. *Bioresour. Technol.* 362, 127790 <https://doi.org/10.1016/j.biortech.2022.127790>.
- Leonard, W., Zhang, P., Ying, D., Fang, Z., 2020. Application of extrusion technology in plant food processing by-products: an overview. *Compr. Rev. Food Sci. Food Saf.* 19, 218–246. <https://doi.org/10.1111/1541-4337.12514>.
- Li, R., Jia, X., Wang, Y., Li, Y., Cheng, Y., 2019. The effects of extrusion processing on rheological and physicochemical properties of sesbania gum. *Food Hydrocolloids* 90, 35–40. <https://doi.org/10.1016/j.foodhyd.2018.11.048>.
- Liu, T.T., Liu, X.T., Chen, Q.X., Shi, Y., 2020. Lipase inhibitors for obesity: a review. *Biomed. Pharmacother.* <https://doi.org/10.1016/j.biopha.2020.110314>.
- Liu, X., Le Bourvellec, C., Renard, C.M.G.C., 2020. Interactions between cell wall polysaccharides and polyphenols: effect of molecular internal structure. *Compr. Rev. Food Sci. Food Saf.* <https://doi.org/10.1111/1541-4337.12632>.
- Menis-Henrique, M.E.C., Scarton, M., Piran, M.V.F., Clerici, M.T.P.S., 2020. Cereal fiber: extrusion modifications for food industry. *Curr. Opin. Food Sci.* 33, 141–148. <https://doi.org/10.1016/j.cofs.2020.05.001>.
- Nogueira Soares Souza, F., Rocha Vieira, S., Leopoldina Lamounier Campidelli, M., Abadia Reis Rocha, R., Milani Avelar Rodrigues, L., Henrique Santos, P., de Deus Souza Carneiro, J., Maria de Carvalho Tavares, I., Patrícia de Oliveira, C., 2022. Impact of using cocoa bean shell powder as a substitute for wheat flour on some of chocolate cake properties. *Food Chem.* 381 <https://doi.org/10.1016/j.foodchem.2022.132215>.
- Oladiran, D.A., Emmambux, N.M., 2018. Nutritional and functional properties of extruded cassava-soy composite with grape pomace. *Starch/Stärke* 70, 1–11. <https://doi.org/10.1002/star.201700298>.
- Punia Bangar, S., Sharma, N., Singh, A., Phimolsiripol, Y., Brennan, C.S., 2022. Glycaemic response of pseudocereal-based gluten-free food products: a review. *Int. J. Food Sci. Technol.* <https://doi.org/10.1111/ijfs.15890>.
- Rani, P., Kumar, A., Purohit, S.R., Rao, P.S., 2018. Impact of fermentation and extrusion processing on physicochemical, sensory and bioactive properties of rice-black gram mixed flour. *LWT-Food Sci. Technol.* 89, 155–163. <https://doi.org/10.1016/j.lwt.2017.10.050>.
- Rebollo-Hernanz, M., Aguilera, Y., Martín-Cabrejas, M.A., Gonzalez de Mejia, E., 2022b. Phytochemicals from the cocoa shell modulate mitochondrial function, lipid and glucose metabolism in hepatocytes via activation of FGF21/ERK, AKT, and mTOR pathways. *Antioxidants* 11, 136. <https://doi.org/10.3390/antiox11010136>.
- Rebollo-Hernanz, M., Zhang, Q., Aguilera, Y., Martín-Cabrejas, M.A., de Mejia, E.G., 2019. Cocoa shell aqueous phenolic extract preserves mitochondrial function and insulin sensitivity by attenuating inflammation between macrophages and adipocytes *in vitro*. *Mol. Nutr. Food Res.* 63, 1801413 <https://doi.org/10.1002/mnfr.201801413>.
- Rebollo-Hernanz, M., Cañas, S., Braojos, C., Cano-Muñoz, P., Martín-Cabrejas, M.A., 2022a. Cocoa shell: Source of novel bioactive ingredients for the prevention of cardiometabolic diseases. In: Campos-Vega, R., Oomah, B.D. (Eds.), *Molecular Mechanisms of Functional Food*. Wiley, Hoboken, NJ, USA, pp. 485–519. <https://doi.org/10.1002/9781119804055.ch15>.
- Rebollo-Hernanz, M., Cañas, S., Taladrí, D., Bartolomé, B., Aguilera, Y., Martín-Cabrejas, M.A., 2021. Extraction of phenolic compounds from cocoa shell: modeling using response surface methodology and artificial neural networks. *Sep. Purif. Technol.* 270, 118779 <https://doi.org/10.1016/j.seppur.2021.118779>.
- Rocchetti, G., Gregorio, R.P., Lorenzo, J.M., Barba, F.J., Oliveira, P.G., Prieto, M.A., Simal-Gandara, J., Mosele, J.I., Motilva, M.J., Tomas, M., Patrone, V., Capanoglu, E., Lucini, L., 2022. Functional implications of bound phenolic compounds and phenolics–food interaction: a review. *Compr. Rev. Food Sci. Food Saf.* 21, 811–842. <https://doi.org/10.1111/1541-4337.12921>.
- Rodríguez-Rodríguez, P., Ragusky, K., Phuthong, S., Ruvira, S., Ramiro-Cortijo, D., Cañas, S., Rebollo-Hernanz, M., Morales, M.D., López de Pablo, Á.L., Martín-Cabrejas, M.A., Arribas, S.M., 2022. Vasoactive properties of a cocoa shell extract: mechanism of action and effect on endothelial dysfunction in aged rats. *Antioxidants* 11. <https://doi.org/10.3390/antiox11020429>.
- Santos, D., Pintado, M., Lopes da Silva, J.A., 2022. Potential nutritional and functional improvement of extruded breakfast cereals based on incorporation of fruit and vegetable by-products - a review. *Trends Food Sci. Technol.* 125, 136–153. <https://doi.org/10.1016/j.tifs.2022.05.010>.
- Schmid, V., Trabert, A., Schäfer, J., Bunzel, M., Karbstein, H.P., Emin, M.A., 2020. Modification of apple pomace by extrusion processing: studies on the composition, polymer structures, and functional properties. *Foods* 9, 8–10. <https://doi.org/10.3390/foods9101385>.
- Soares, T.F., Oliveira, M.B.P.P., 2022. Cocoa by-products: characterization of bioactive compounds and beneficial health effects. *Molecules* 27, 1625. <https://doi.org/10.3390/molecules27051625>.
- Taladrí, D., Rebollo-Hernanz, M., Martín-Cabrejas, M.A., Moreno-Arribas, M.V., Bartolomé, B., 2023. Grape pomace as a cardiometabolic health-promoting Ingredient: Activity in the intestinal environment. *Antioxidants* 12 (4), 979. <https://doi.org/10.3390/antiox12040979>.
- Villasante, J., Pérez-carrillo, E., Heredia-olea, E., Metón, I., Almajano, M.P., 2019. *In vitro* antioxidant activity optimization of nut shell (*Carya illinoensis*) by extrusion using response surface methods. *Biomol* 9 (883 9), 883. <https://doi.org/10.3390/Biom9120883>, 2019.
- Wang, C., Liu, Y., Xu, L., Xin, C., Tan, Z., Zhang, X., Ma, C., Chen, S., Li, H., 2022. Changes of the main components, physicochemical properties of distiller's grains after extrusion processing with focus on modification mechanism. *Food Chem.* 390, 133187 <https://doi.org/10.1016/j.foodchem.2022.133187>.
- Yi, C., Qiang, N., Zhu, H., Xiao, Q., Li, Z., 2022. Extrusion processing: a strategy for improving the functional components, physicochemical properties, and health benefits of whole grains. *Food Res. Int.* <https://doi.org/10.1016/j.foodres.2022.111681>.
- Zhang, R., Khan, S.A., Chi, J., Wei, Z., Zhang, Y., Deng, Y., Liu, L., Zhang, M., 2018. Different effects of extrusion on the phenolic profiles and antioxidant activity in milled fractions of brown rice. *LWT-Food Sci. Technol.* 88, 64–70. <https://doi.org/10.1016/j.lwt.2017.09.042>.
- Zhu, Y., Ji, X., Yuen, M., Yuen, T., Yuen, H., Wang, M., Smith, D., Peng, Q., 2021. Effects of ball milling combined with cellulase treatment on physicochemical properties and *in vitro* hypoglycemic ability of sea buckthorn seed meal insoluble dietary fiber. *Front. Nutr.* 8, 820672 <https://doi.org/10.3389/fnut.2021.820672>.